

# Effect of pH on structural and magnetic properties of Pr-Co substituted Strontium Hexaferrite

A dissertation report

Submitted

By

**Sonam Chauhan**

To



Department of Physics

In partial fulfilment of the requirement for the

Award of the Degree of

Master of Science

Under the guidance

of

**Dr. A. K. Srivastava**

Phagwara, Punjab

3 May, 2015

## DECLARATION

I hereby declare that the dissertation report entitled, “**Effect of pH on structural and magnetic properties of Pr-Co substituted Strontium Hexaferrite**” submitted for the M.Sc.(Hons) Physics degree is entirely my original work and all ideas and references have been duly acknowledged. It does not contain any work for the award of any other degree or diploma at any university.

Sonam Chauhan

M.Sc (H) Physics

11302052

## CERTIFICATE

This is to certify that Ms. Sonam Chauhan has completed the dissertation report entitled “**Effect of pH on structural and magnetic properties of Pr-Co substituted Strontium Hexaferrite**” under my guidance and supervision. To the best of my knowledge, the present work is the result of her original investigation and study.

Date: 3 May, 2015

Name: Dr. A. K. Srivastava

Designation: Assistant Professor

Department of Physics

Lovely Professional University, Phagwara.

## **ACKNOWLEDGEMENT**

I would like to express my sincere gratitude and indebtedness to my supervisor Dr. A.K. Srivasatva, Assistant Professor, Department of Physics, Lovely Professional University (Phagwara) for his invaluable advice, constant encouragement and wholehearted cooperation throughout the course of this research work.

I also wish to place on my deep debt of gratitude to Mr. Parminder Singh (Lab.technician Physics) for providing me apparatus and other facilities to carry out reach work.

My special thanks to Mrs. Talwinder Kaur (student of Phd) for her heartiest support to me, and giving tips regarding this study. In giving appreciation, I must acknowledge my parents for their unwavering love, support and help to accomplish this study.

Last but not least, I would like to thank Lovely Professional University for giving me an opportunity to be a part of this research work.

Sonam Chauhan

11302052

## CONTENTS

<b>S.N.</b>	<b>Chapters</b>	<b>Pages</b>
1	Introduction	6-9
2	Scope Of The Study	10
3	Objectives Of The Study	11
4	Review Of Literature	12-17
5	Equipment, Materials, and Experimental Setup	18-19
6	Research Methodology	20-21
7	Results and discussion	22-33
8	Summary And Conclusions	34
9	List of References/Bibliography	35-37
10	Abstract	38

The properties of nano materials, made from nano particles are different from bulk materials. Now-a-days the chief attention is on the construction of nano particles. There is a great importance for the preparation of ferrite in nanorange to meet the nanotechnology: Nanotechnology can be defined as design, manufacture and application of nanomaterials, and it also gives the important accepting of the connections between the physical belongings and measurements of particles. It agreements with materials in nanometer scales ( $10^{-9}$  m). This technology also gives the possibility of creating nanostructures of metastable stages with belongings like superconductivity and magnetism. There is extra significance of nanotechnology.

One of the major advances in the field of nanotechnology is the development of ferrite materials, which because of their remarkable magnetic behavior prove to be useful in many modern day applications such as ferrite cores, ferrite magnets and in microwave devices. Researchers, over a period of time have been keenly interested in the sphere of ferrites and many successful attempts have been made to synthesize ferrite materials that show improved magnetic properties such as saturation magnetization, anisotropy constants etc for better use in applications. Ferrites are deliberated much improved than the other magnetic tools as they have small eddy current losses and have high electrical resistivity. M –type hexaferrite having formula  $MFe_{12}O_{19}$ , where M can be Sr, Pb, Ba have been a question of attention because these compounds have been the work mount of long-lasting magnet fair. Strontium hexaferrite has been studied for magneto-optical recording and magnetic recording media. They are ferromagnetic as they can be magnetized or attached to a magnet also they are electrically nonconductive. Ferrites can be divided into two classes based on magnetic coercivity, resistance to being demagnetized.

### 1.1: SOFT FERRITES

Soft ferrites are those which have low coercivity. Low coercivity states that the materials magnetization can effortlessly reverse direction without dispersing significantly energy though the materials great resistivity avoids eddy current loss in the core. RF transformers and inductors uses the soft ferrites. Examples: zinc ferrite, Nickel ferrite.

## 1.2: HARD FERRITES

Hard ferrites are those which have high coercivity and great remanence. Permanent magnets that are equipped of the hard ferrites, as hard ferrites have the great coercivity & great remanence when magnetize. Mainly Iron oxide and strontium carbonate are used to manufacture the hard ferrite. The great coercivity funds that the materials are very tough to becoming demagnetized. It is an necessary unambiguous for a permanent magnet. They also have permeability. Examples: strontium ferrite, barium ferrite.

### **TYPES OF HEXAFERRITES:**

#### (i)THE W FERRITES

General formula of W type ferrites is  $BaMe_2Fe_{16}O_{27}$ , where Me is the D block elements or the particular divalent cation and the barium that could be replaced by additional group elements. All W type ferrites ensure uniaxial anisotropy, exception is  $Co_2W$  ferrite having formula ( $BaCo_2Fe_{16}O_{27}$ ), and the molecular mass of 1581 g and the density  $5.31gcm^{-3}$ . It has a cone of informal magnetization at constant angle  $70^\circ$  to c- axis from the  $-273^\circ C$ , at which the point, its anisotropy revolves to the c-axis with the growing temperature till it converts uniaxial at the temperature of  $280^\circ C$ , and the magnetization becomes constant in the c-axis with additional rise in the temperature.

#### (ii)THE M FERRITES:

General formula of M type ferrite is BaM,  $BaFe_{12}O_{19}$ . The melting point of M type ferrite is  $1390^\circ C$  confirmed in the year of 1936. Though, the structure of M type ferrite had not established as existence of isomorphous with the hexagonal magneto - plumbite till it had been considered and characterized magnetically by Philips in 1950. It was deliberated as the unfamiliar ferrites as per it was confined with no nickel and cobalt, however this was attractively firm with the coercivity of 160-255kA/m. They were very inexpensive to yield and had a great electrical resistivity of  $10^8$  cm and also it has great magnetic uniaxial anisotropy beside the c-axis. BaM having molecular mass of 1112 g and the determined density is of  $5.295gcm^{-3}$ , even though in the certainty a ceramic material repeatedly which had a density less then 90% of

hypothetical density. Rigidity of the BaM in the c-axis had been measured to be 5.9 GPa and dignified as 6.0Pa.

(iii)THE X FERRITE:

The X ferrites were first described in the year of 1952 as they had varied phase of M and W ferrite. The general chemical formula of X ferrites is  $Ba_2Me_2Fe_{28}O_{46}$ , in which Me is the D block element or the certain divalent cation. First described X ferrite is the  $Fe_2X$ ,  $Me = Fe^{2+}$  and this was establish that it had the uniaxial magnetic anisotropy beside a c- axis. The density is of  $5.3gcm^{-3}$ . Totally X ferrites have the uniaxial anisotropy at RT, exception is the  $Co_2X$ , it had cone of magnetization (at  $74^\circ$ ) to the c- axis. Alike W ferrite they appear like, the cone vagaries to implement an alignment parallel to the c-axis at the greater temperature,  $143^\circ C$  in this saturation.

(iv)THE Y FERRITES:

The first ferroplana ferrites to be exposed, is Y ferrite and currently identified as almost all Y ferrites had the favored plane of magnetization upright to the c-axis at RT. General formula for the Y ferrites is the  $Ba_2Me_2Fe_{12}O_{22}$ , where Me is the small divalent cation, and  $Zn_2Y$  and  $Co_2Y$  were the first made for ferrites.  $Co_2Y$  have molecular mass of 1410 g, and having density  $5.40 g cm^{-3}$ . At RT, the  $Co_2Y$  has planer anisotropy but it fluctuations to cone of magnetization below  $-58^\circ C$ . the temperature from  $-58^\circ C$  to the curie point, the anisotropy rests in favored plane. The  $Cu_2Y$  is the single Y ferrites which were initiate to had a desired the uniaxial way of the magnetization.

(v)THE Z FERRITES:

The general formula of Z ferrites are  $Ba_3Me_2Fe_{24}O_{41}$ . They are exposed at that period as the ferroplana Y ferrites were found. Molecular mass of  $Co_2Z$  is 2522g and it has  $5.35g cm^{-3}$  density. Entirely Z ferrite have the uniaxial anisotropy parallel to the c-axis, exception is the  $Co_2Z$ , as it is a planar at RT but then it has the composite magnetic anisotropy, atleast 4 dissimilar anisotropic positions. At small temperatures the  $Co_2Z$  had informal cone of magnetization, at the angle of  $65^\circ$  to the c-axis, and it always constant up to  $-103^\circ C$ . Between  $-103^\circ C$  and  $-53^\circ C$  angle rises to the  $90^\circ$ , and the desired magnetization remnants in the basal plane



till this changes to the c-axis at a certain high temperature sandwiched between 206 degree and 242°C.

(vi) THE U FERRITES:

The general formula of U ferrites are  $Ba_4Me_2Fe_{36}O_6$ . Though it is recognized at the similar time as additional hexagonal ferrites. The U ferrites had been not characterised greatly both magnetically or structurally. 5.44 is the density of  $Co_2U$  and the density of the  $Zn_2U$  is 5.31 g  $cm^{-3}$ . The U ferrites are having uniaxial anisotropy exception is the  $Co_2U$ , which are having planar anisotropy at RT, and molecular mass of the  $Co_2U$  is 3622 g.

### 1.5: APPLICATIONS OF HEXAFERRITES

The hexaferrites have many applications, like in motors, transformers, generators, sensors, information storage, mobile communications, security, and transport, aerospace and to focus the electron beams. The ferromagnetic materials are the mostly used magnetic material. Alloys or ferromagnetic ceramics are also used mostly.

- 1) Permanent magnet
- 2) Number of applications like Medical devices, Microwave ovens, laptops, telecommunications like Phones and T.V

Devices of Gyromagnetic electronics: Filters, Absorbers for computers and other electronics as in Circulator and Power meters.

The synthesized compounds can be used in many applications like permanent magnets, medical devices, microwave ovens, computers, local communications, phones and T.V, circulator, filters, power meters, absorbers for computers and other electronics.

In the present research work, we have synthesized Pr-Co substituted strontium hexaferrite at different pH value using sol gel auto combustion method. The structural, thermal and magnetic properties are studied by XRD, FTIR, TGA and VSM.

Hasab et al. (2007) have adopted the sol-gel technique to make the strontium hexaferrite nanoparticles using metal nitrates and ammonia which is used to adjust the pH. Reagent n-decyltrimethylammonium bromide is used as the cationic surfactant and citric acid, acetyl acetone, glycine and oxalic acid are used as fuels. Temperature form the hexaferrite and the crystallite size in the existence of dissimilar fuels had compared together. The results had showed the smallest crystallite size 37.3nm and lowest formation temperature in the existence of citric acid was 900<sup>0</sup>C.

**Jotania et al. (2008)** have prepared the W-type hexaferrite nanoparticles with composition of  $B_2C_{12}F_1O_2$  by microemulsion technique and auto combustion method with and without surfactants at several sintering temperatures. X-ray Diffraction is used to study the structural properties, VSM is used to study the magnetic properties, Scanning Electron Microscopy is used to analyse the surface features, thermal properties were studied by Thermogravimetric analysis Differential Scanning Calorimetric (DSC) and Fourier Transform Infrared Spectroscopy (FTIR) is used to detect the chemical group that are attached to the formed powder. Magnetization was depend on the surfactant used. Sample which prepared in presence of polyoxyethylene (20) sorbitan monooleat showed small saturation magnetization and the sample which formed in the occurrence of a surfactant cetyltrimethylammoniumbromide (CTAB) exhibited the extraordinary saturation magnetization as compared to the normal samples .

**Bsoul and Mahmood (2009)** studied the structural and magnetic properties of  $(BaFe_{12-x}Ga_xO_{19})$  nanoparticles with varying x from 0 to 1.0. The samples have been prepared by the technique of ball milling and are studied using XRD, VSM and TEM. It was found that the particles and the crystallites have same average size of 41nm approximately for wholly samples which are examined. The  $M_s$  was reduced a little and nonlinearly with the increasing x, and it was recognized to the dissimilar preferential site occupation of the Ga at high and low concentration

ranges. The  $H_c$  was reduced marginally with growing value of ( $x$ ) for small concentrations of Ga,  $x$  is less than or equal to 0.2 and then better with the increase Ga concentration up to the value  $x = 1$ .

**Junliang *et al.* (2009)** have synthesized the quasi- single domain M-type barium hexaferrite powders using the technique of sol-gel. The effects of citric acid on the metal ions and the pH values on the sol gel, phase configurations of the created powders and the magnetic properties are calculated. They found that chelation of the barium and the ferrite ions was important for the phase realization of the barium hexaferrite; the phase compositions of the prepared particles different from a multi-phased mixture to a single phase of ( $M-B F_1 O_1$ ) for the gradual complete complexing of the barium and the iron ions with citrate as pH values and metal ion were increased.

**Iqbal *et al.* (2009)** have prepared the Y-type hexagonal ferrites of the nominal composition ( $B_2C_2(Z)_{x-2x}F_1-2xO_2$ ) by the technique of sol-gel. The XRD patterns of samples have showed a micrographs and crystalline nature of the samples with undeviating particle dimension spreading. Crystallite extent distribution of samples was deliberate of range of 46nm-59nm. The resistivity of samples decreased on growing temperature but increased on the increasing Zr-Co contented. The Doping of Zr-Co significantly affected lattice c-parameter, the crystallite size, the Curie temperature, the DC resistivity, and drift mobility.

**Iqbal and Farooq (2010)** synthesized and characterized ( $S_{0.5}B_{0.5-x}P_xF_1-yN_yO_1$ ) hexaferrite nanomaterial. XRD results had showed specific peaks of the magnetoplumbite structure for taken compounds. Values of  $M_s$  was establish to rise in the range of 65-78 and remanence was establish to rise in the ranges of 43-48 emu/g. The coercivity was found to be contrariwise allied to the Pr-Ni contents. AC magnetic susceptibility studies have showed the piercing ferri to paramagnetic transition in range of 500-672K temperature.

**Liu. et al. (2010)** have prepared a sequence of powders of the M-type barium hexaferrites doped with some elements like Zn, Sn and Co with formula  $(B F_{1-2x}Z_{x/2}C_{x/2}S_xO_1)$  with x equal 0 to 2 by co precipitation process. The structural property was characterised by X-ray powder diffraction ,particle morphology was characterised by SEM and the vibrating sample magnetometer is used to analyse the magnetic properties. The results after characterization showed that the crystallinity of the sample falls with the rise in the doping volume of x. A high saturation magnetization and a temperature dependence of coercivity was close to zero for doped barium hexaferrites when the value of x lies between 0.3 and 0.4.

**Singhal et al. (2011)** have prepared M-type hexaferrites  $MF_1O_1$  and the  $M F_1 O_1$  where M can be Ba Sr and Pb by technique of autocombustion process to examine shielding influence of the inorganic ions like KBr, KCl and KI on phase progression of hexaferrites. The FTIR frequency bands are detected in frequency range  $560 - 580 \text{ cm}^{-1}$  and  $430 - 470 \text{ cm}^{-1}$ . X-ray diffractographs not show any peaks for obtained samples, showing amorphous nature of the samples, but regular peaks for M-type structure were found for annealed samples. Negligibly change in the lattice constant 'a' and 'c' was noted with replacement of Al in hexagonal ferrite. Magnetic dimensions showed that value of coercivity for whole the samples with KCl and KBr improved as KCl and KBr acted as a deactivators. The value of coercivity reduced with KI replacement as it oxidized to  $I_2$  in hardening. The saturation magnetization of hexaferrites decreased with  $A^{+3}$  ion substitution for  $F^{+3}$  ion due to preferential occupancy of  $A^{+3}$  ion in the octahedral sites.

**Davoodi and Hashemi (2011)** synthesized Sn-Mg relieved strontium hexaferrite with configuration of  $SrFe_{12-x}(Sn_{0.5}Mg_{0.5})_xO_{19}$  (x=0-1) by method of chemical co precipitation. Deionized water 50/50 was used as the solvent. The only phase hexaferrites were achieved at the pH of 13 and the  $Fe^{3+}/Sr^{2+}$  molar ratio of nine after animated at the temperature of 800°C. With growing the Sn-Mg contents from (x=0 to x=0.8) the average particle size of the samples was reduced from 82 to 56nm. The magnetic properties of the hexaferrites are calculated using the VSM. On increasing the Sn-Mg from x=0 to x=0.8 it reduced the  $H_c$  from the value of 4728.9 to

1455.5Oe and increased saturation magnetization( $M_s$ ) from 51.34 to 65.49emu/g. A method called the vector network analyzer was used to examine the microwave absorption properties. According to the microwave quantities, it had been instigate that doped the taken hexaferrite composites had more operative electromagnetic absorption properties than the undoped hexaferrite.

**Nakamura et al.** (2012) studied that the Y- type hexaferrite having composition ( $Ba_2Mg_2Fe_{12}O_{22}$ ) had been conducted with the single crystal specimen. The spins were in the c-plane down to 60 K. For transition from the ferromagnetic to proper screw spin structure takes. At temperature 16 k, the spins inclined about 15degree from the c-plane. Below the temperature 50K, the spin reorientation transition to the longitudinal conical structure was also predictable.

**Wang et al.** (2013) prepared strontium ferrite with  $Nd^{3+}$ ,  $Al^{3+}$  and  $Ca^{2+}$  substitution of  $Fe^{3+}$  and  $Sr^{2+}$  ions by the conventional solid phase reaction process. The  $Nd^{3+}$  substitution shows 10 % – 20 % improvement in coercivity for the substitution content less than 10 %. The  $Ca^{2+}$  substitution is favorable to the enhancement of saturation magnetization due to the accelerated reaction of  $Fe_2O_3$  and  $SrCO_3$ . The samples with  $Al^{3+}$  substitution of  $Fe^{3+}$  show the lowest saturation magnetization, although the highest coercivity was achieved for a homogeneous grain size less than 1  $\mu m$ . The combinatory substitution  $Nd^{3+}$ ,  $Ca^{2+}$  and  $Al^{3+}$  leads to the optimum magnetic properties with  $s = 52 \text{ Am}^2/\text{kg}$  and  $H_{cj} = 412 \text{ kA/m}$ .

**Fenfang Xu et al.** (2014) synthesized the composite of chiral polyaniline (PANI)/barium hexaferrite (BF) by in situ polymerization using L-camphorsulfonic acid as chiral dopant. The structural features of the obtained composites were characterized by FTIR, XRD and FESEM techniques. Open circuit potential was measured in D-/L-alanine electrolyte in order to identify the chirality of the composite. Microwave absorbing properties were investigated by measuring complex permittivity and complex permeability in the frequency range of 26.5–40 GHz. As a result, chiral PANI/BF composite exhibited excellent microwave absorbing properties with the

minimum reflection loss of 30.5 dB at 33.25 GHz with a thickness of only 0.9 mm, and the absorption bandwidth of the reflection loss below  $-10$  dB could reach 12.8 GHz (from 26.5 to 39.3 GHz), which almost covered the whole Ka band (26.5–40 GHz). The enhanced microwave absorbing properties were attributed to the helical structural characteristic and the good impedance matching between BF particles and chiral PANI.

**Talwinder Kaur et al.** (2015) synthesized M-type barium hexaferrite  $[\text{Ba}_{1-x}\text{Nd}_x\text{Co}_x\text{Fe}_{12-x}\text{O}_{19}$  ( $x = 0.0-0.5$ ) (BNCM)] powders, using the technique of citrate precursor method. When the pattern of powders was subjected to X-ray diffraction, it shows the formation of M-type hexaferrite phase. The formation of sample is observed to be at  $440^\circ\text{C}$  as per the analysis of thermogravimetric analysis/differential thermal analysis/derivative thermogravimetry. The presence of two prominent peaks near  $430$  and  $580\text{ cm}^{-1}$  in FTIR spectra indicates the formation of M-type hexaferrites. The saturation magnetization, retentivity, squareness ratio and coercivity were calculated by M-H curve obtained from VSM. UV–Vis NIR spectroscopy had given that band gap depends on size of the crystallites. At low frequency, the dielectric constant is found to be high and decreases with increase in frequency. This kind of behaviour is described on basis of the Koop's phenomenological theory and the Maxwell–Wagner theory.

**Talwinder Kaur et al.** (2015) synthesized M-type barium hexaferrite  $\text{Ba}_{0.7}\text{La}_{0.3}\text{Fe}_{11.7}\text{Co}_{0.3}\text{O}_{19}$  powder, using sol gel method, which is heated at different temperatures  $700$ ,  $900$ ,  $1100$  and  $1200^\circ\text{C}$ . The X ray diffraction (XRD) powder patterns of the heated samples show the foundation of pure phase of M-type hexaferrite after the temperature of  $700^\circ\text{C}$ . The Thermo gravimetric analysis shows that weight loss of synthesized sample becomes constant after the temperature of  $680^\circ\text{C}$ . The existence of two prominent peaks, at  $432\text{ cm}^{-1}$  and  $586\text{ cm}^{-1}$  in FT-IR spectra, gives the info of the formation of M-type hexaferrites. The saturation magnetization, retentivity, squareness ratio and coercivity were calculated by M-H curve obtained from VSM. The maximum value of coercivity ( $5602\text{ Oe}$ ) is originated at temperature of  $900^\circ\text{C}$ . The dependency of band gap on temperature was calculated by using UV–vis NIR spectroscopy. At low frequency, the dielectric constant is found to be high however it decreases with increase in



frequency. Such kind of dielectric behavior is described on basis of the Koop s phenomenological theory and the Maxwell Wagner theory.

## CHAPTER 5 EQUIPMENTS, MATERIALS AND EXPERIMENTAL SETUP

---

Strontium nitrate ( $\text{Sr}(\text{NO}_3)_2$ ), praseodymium nitrate ( $\text{Pr}(\text{NO}_3)_3 \cdot 6\text{H}_2\text{O}$ ), cobalt nitrate ( $\text{Co}(\text{NO}_3)_2 \cdot 6\text{H}_2\text{O}$ ), ferric nitrate ( $(\text{Fe}(\text{NO}_3)_3)_3 \cdot 9\text{H}_2\text{O}$ ), citric acid pure ( $\text{C}_6\text{H}_8\text{O}_7 \cdot \text{H}_2\text{O}$ ) and ammonia solution are used for the synthesis of Pr-Co substituted strontium hexaferrite. Following instruments are used to know the properties of synthesized hexaferrites:

- X-ray Diffraction:

X-ray diffraction (XRD) method is the best operative method to define the crystal structures of the materials. X-ray diffraction can also identify the chemical compounds. but it cannot identify the chemical compound from their compositions.

- Fourier Transform Infrared Spectroscopy:

Fourier Transform Infrared Spectroscopy also called FT-IR, is the best used and mostly vibrational spectroscopy method. It uses the infrared spectroscopy transform technique called fourier transform which is used to acquire an infrared spectrum in a entire range of the wavenumbers instantly. The chief component in the FTIR system is the Michelson interferometer.

- Thermogravimetry Analysis(TGA)

Thermal Analysis (TA) is a collection of systematic techniques that measure properties or property changes of materials as a function of temperature. Changes in materials properties with temperature are measured as thermal events. The most commonly used thermal analysis techniques for materials characterization are: Thermogravimetry (TG), Differential Thermal Analysis (DTA) and Differential Scanning Calorimetry (DSC). Thermogravimetric analysis is the most commonly used thermal method. It is based on the mass loss of material as a the function of temperature.

In TGA a continuous graph of mass change against temperature is obtained when a substance is heated at a uniform rate or at a constant temperature. A graph plot between mass change and temperature (T) is known as Thermogravimetric curve. There are many

applications of thermogravimetry analysis like purity and thermal stability, solid state reaction and determining moisture, volatile and ash contents

- Vibrating sample magnetometer:

A vibrating sample magnetometer (VSM) works on Faraday's law of induction, which says that a changing magnetic field will produce an electric field. This electric field can be calculated and can tell us the information around the changing magnetic field. A VSM is used to measure the magnetic behavior of magnetic materials.

There is an important aspect about nanoferrites that their behavior like magnetic properties depends commonly on the grain size and phase purity which are much affected by the synthesis techniques. There are many methods to synthesize nanoferrites which include the traditional ceramic sintering route, mechanical grinding, the micro-emulsion technique, the hydrothermal reaction, the glass crystallization technique like sol-gel technique, salt-melt technique etc.

Nowadays the most commonly used method is the sol-gel method. It has been used for the preparation of nano grained hexaferrites. Main advantages of this method are:

- low cost
- energy efficiency and
- high production rate.
- Lower calcination temperature
- Ultrafine resultant particles

Also, sol- gel method provides a multi component oxide with a homogenous composition as in sol-gel method the amount of reactants can be easily controlled.

### **6.1 Sample preparation steps and chemical used**

We have synthesized Pr-Co substituted strontium hexaferrite using AR grade nitrates, citric acid and ammonium solution. We have adopted sol gel auto combustion method. In this method, first of all, nitrates and citric acid are dissolved in distilled water and then mixed together. The pH of the solution is maintained by ammonium solution. The mixtures are heated at 80<sup>0</sup>C for 4 hours at magnetic stirrer and then heated at 280<sup>0</sup>C in a hot plate for 3 hours. The samples are pre-calcined at 500<sup>0</sup>C for 2 hour and then calcined at 900<sup>0</sup>C for 4 hours (Fig. 6.1).

### **6.2. Chemical required to synthesizing the strontium hexaferrites**

- Strontium nitrate AR grade [ $\text{Sr}(\text{NO}_3)_2$ ] : 0.5079g/mol
- Praseodymium nitrate AR grade [ $\text{Pr}(\text{NO}_3)_3 \cdot 6\text{H}_2\text{O}$ ] : 0.6960g/mol
- Cobalt nitrate AR grade [ $\text{Co}(\text{NO}_3)_2 \cdot 6\text{H}_2\text{O}$ ] : 0.4656 g/mol
- Ferric nitrate GR grade [ $(\text{NO}_3)_3 \cdot 9\text{H}_2\text{O}$ ] : 18.7456g/mol
- Citric acid anhydrous [ $\text{C}_6\text{H}_8\text{O}_7 \cdot \text{H}_2\text{O}$ ] : 21.8546 g/mol
- Liquor ammonia [AR grade] to control the pH of the initial solution between 2 to 10.47.

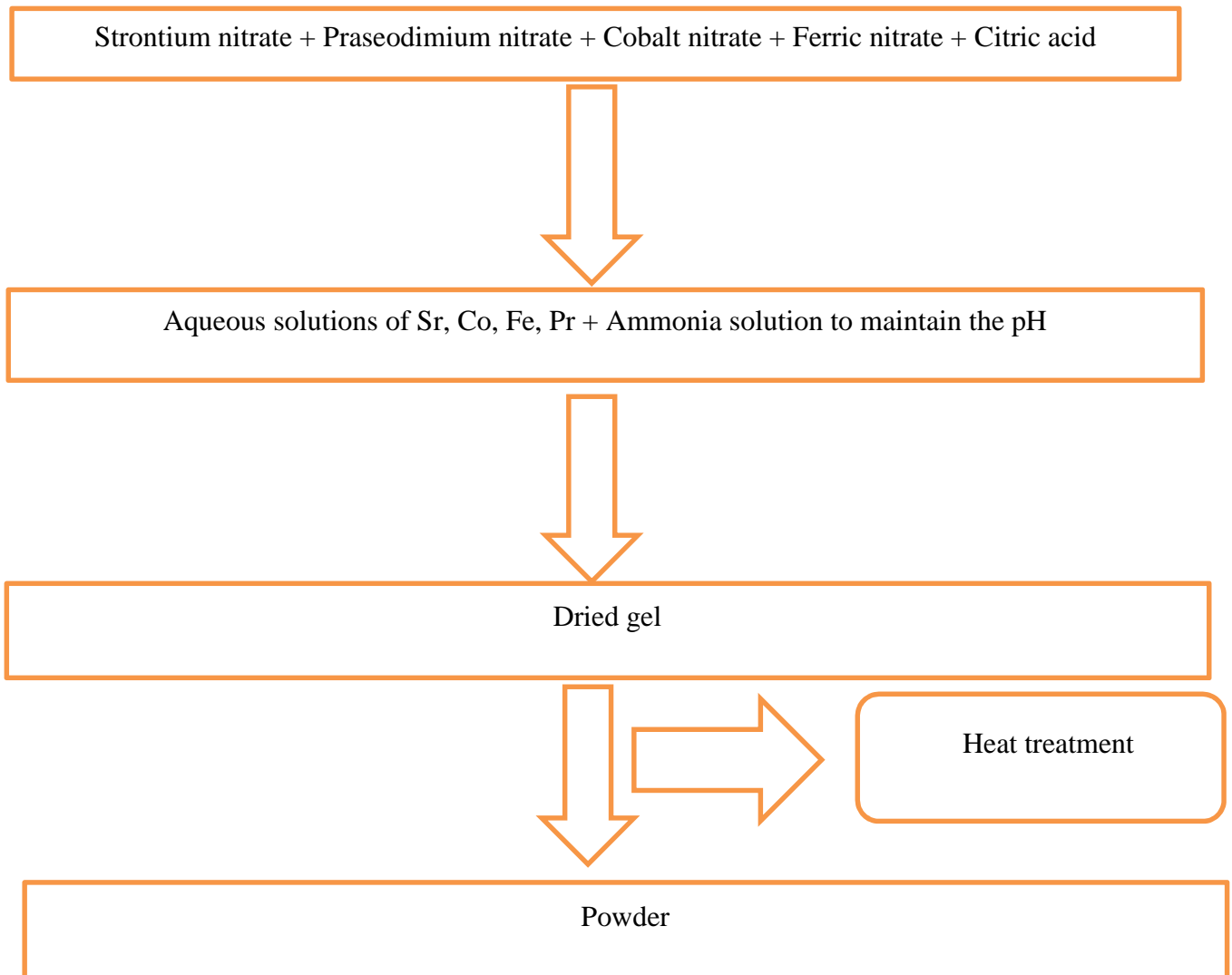


Fig.6.1:Flow chart of steps

### 7.1.X-RAY DIFFERACTATION (XRD)

The X-ray diffraction had been carried out by using *CuK $\alpha$*  radiation ( $\lambda=1.54060\text{\AA}$ ) with a Paranalytical X-ray diffraction unit. XRD analysis tells that the observed diffraction peaks and miller indices (hkl) for M-type strontium hexaferrite. The diffraction patterns consist of peaks corresponding to crystallographic planes (008), (107), (110), (200), (203), (205), (206), (209), (220), (304) (Figs.7.1-7.5). The grain size ‘D’ is calculated using the Scherrer formula:

$$D=k\lambda/\beta\cos\theta$$

where,  $\lambda$  is the wavelength of X-rays which is equal to  $1.54060\text{\AA}$ ,  $\beta$  is the half peak width,  $\theta$  is the Bragg’s angle and  $k$  is the shape factor that is equal to 1 for hexagonal system. The average grain size is found to be in the range of 27.234-57.455nm (tabulated in **Table 7.1**) for the synthesized samples. The lattice constants ‘a’ and ‘c’ are calculated for prominent peaks (006) and (107) for samples using the equation:

$$\frac{1}{d_{hkl}^2} = \frac{4}{3} \left[ \frac{h^2 + hk + k^2}{a^2} \right] + \frac{l^2}{c^2}$$

The lattice constant “a” first decreases with increase in pH value from 2 to 7 and then increases with increase in pH value from 9 to 10.4. The lattice constant c is same at pH = 2 and 4. At pH=7, lattice constant is found  $23.0659\text{\AA}$  (**Table 7.1**).

And volume of unit cell is calculated from the formula:

$$V_{cell} = 0.866 a^2 c$$

The volume of cell first decreases with increasing pH (From pH=2 to pH=7) then increases with increasing pH (from pH=9 to pH=10.47) (**Table 7.1**).

**Table 7.1:** Average particle size, lattice constants and volume of  $\text{Sr}_{0.6}\text{Pr}_{0.4}\text{Fe}_{11.6}\text{Co}_{0.4}\text{O}_{19}$

pH value	2	d (Å)	(°)	a(Å)	c (Å)	D(nm)	Vol(Å <sup>3</sup> )
2	33.298	2.6885	0.261	5.9191	22.9744	57.455	697.06
4	32.551	2.7485	0.383	5.8902	22.9744	27.346	690.27
7	32.458	2.7562	0.332	5.8622	23.0659	30.671	686.45
9	32.411	2.7601	0.369	5.8901	23.0201	27.234	691.62
10.47	32.364	2.7640	0.322	5.9185	23.0201	28.554	698.31

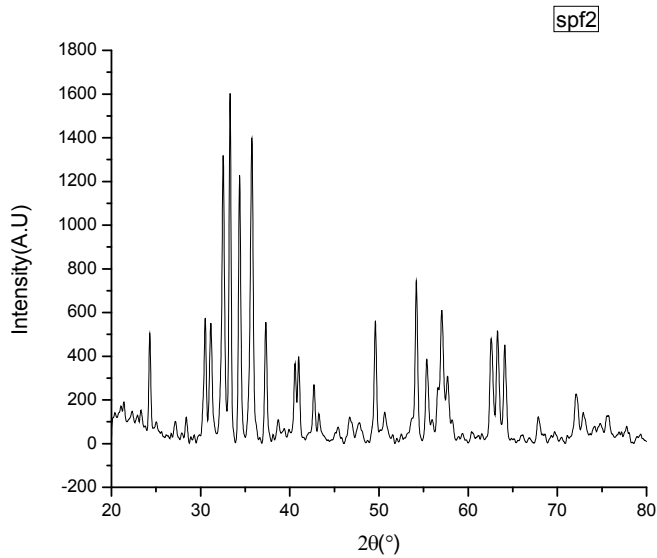


**Fig.7.1:**XRD pattern of  $\text{Sr}_{0.6}\text{Pr}_{0.4}\text{Fe}_{11.6}\text{Co}_{0.4}\text{O}_{19}$  at pH=2

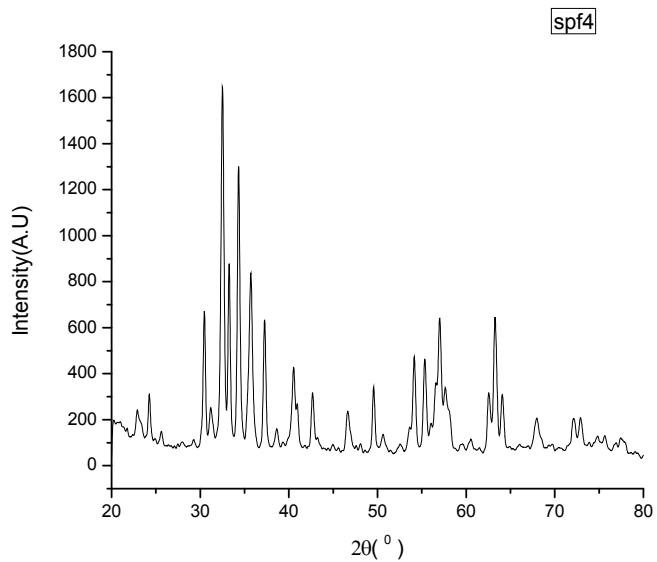


**Fig.7.2: XRD pattern of  $\text{Sr}_{0.6}\text{Pr}_{0.4}\text{Fe}_{11.6}\text{Co}_{0.4}\text{O}_{19}$  at pH=4**

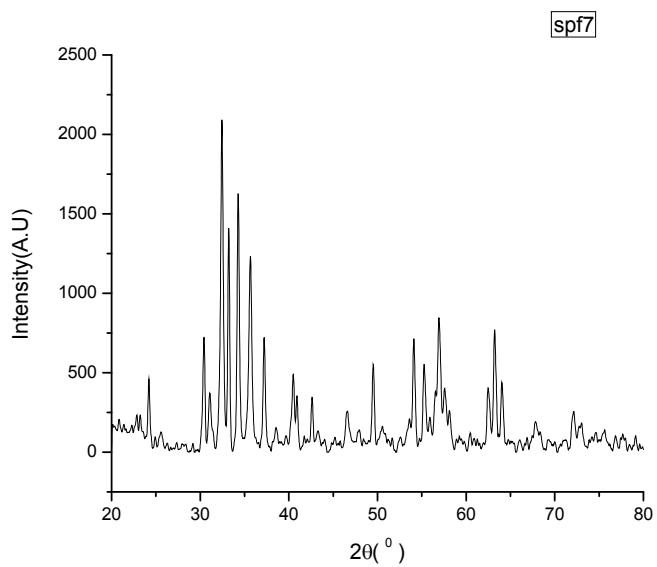


**Fig.7.3: XRD pattern  $\text{Sr}_{0.6}\text{Pr}_{0.4}\text{Fe}_{11.6}\text{Co}_{0.4}\text{O}_{19}$  at pH=7**



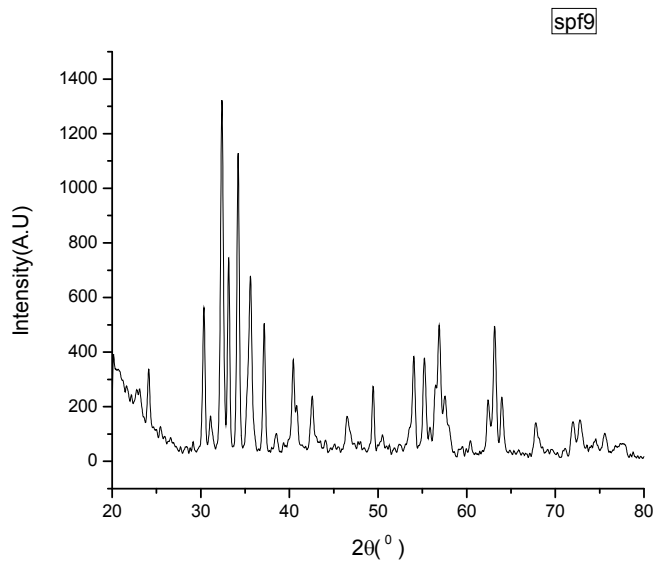


**Fig.7.4:XRD pattern of  $\text{Sr}_{0.6}\text{Pr}_{0.4}\text{Fe}_{11.6}\text{Co}_{0.4}\text{O}_{19}$  at pH=9**

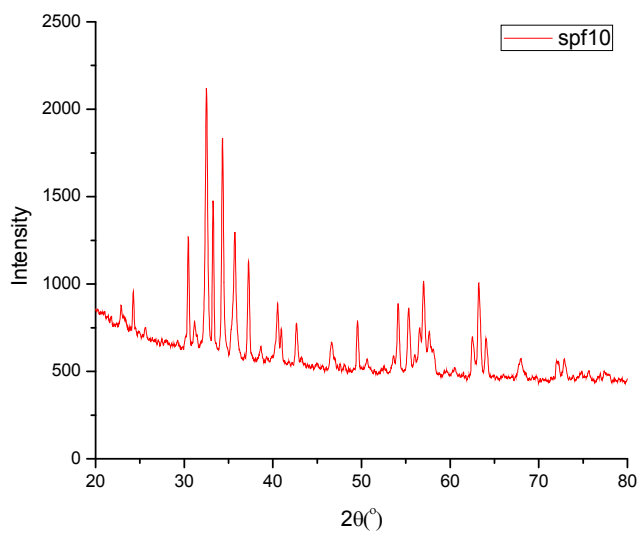


**Fig.7.5:XRD pattern of  $\text{Sr}_{0.6}\text{Pr}_{0.4}\text{Fe}_{11.6}\text{Co}_{0.4}\text{O}_{19}$  at pH=10.47**

## 7.2.VIBRATING SAMPLE MAGNETOMETER:

The magnetic properties of the synthesized samples had been studied by using the Vibrating Sample Magnetometer (VSM) PAR-155 from Princeton Applied Research, USA. Saturation magnetization ( $M_s$ ), retentivity and coercivity ( $H_c$ ) are achieved from the hysteresis curves shown in the figures (Figs.7.6-7.10). The magnetic anisotropy constant ( $K$ ) is related to coercivity ( $H_c$ ) and can be calculated using the relation (Table 7.2):

$$H_c = \frac{2K}{\mu_0 M_s}$$

where  $H_c$  is the coercivity,  $M_s$  is the saturation magnetization and  $\mu_0$  is permeability  $4\pi \times 10^{-7}$  N/A<sup>2</sup>.

It is clear from the hysteresis curves that the saturation magnetization ( $M_s$ ) depends upon the pH of the samples. From the M-H curve, the value of coercivity, saturation magnetization and retentivity are calculated and reported in Table 7.2.

**Table 7.2:** Coercivity, magnetization, retentivity and anisotropic constant( $K$ ) of  $Sr_{0.6}Pr_{0.4}Fe_{11.6}Co_{0.4}O_{19}$

pH value	Coercivity (Oe)	Magnetization (emu/g)	Retentivity (emu/g)	Anisotropic constant( $K$ )
2	1346.1539	3.5208	1.3672	$2.98 \times 10^{-3}$
4	1875.0000	6.9783	2.8979	$8.22 \times 10^{-3}$
7	1466.3461	3.6554	1.4279	$3.37 \times 10^{-3}$
9	5432.6923	3.4707	1.9584	$1.18 \times 10^{-2}$
10.47	5084.1346	4.2023	2.3372	$1.34 \times 10^{-2}$

The highest value of coercivity is 5432.6923 Oe for the sample having pH=9. The maximum value of  $K$  was found to be  $8.22 \times 10^{-3}$ .

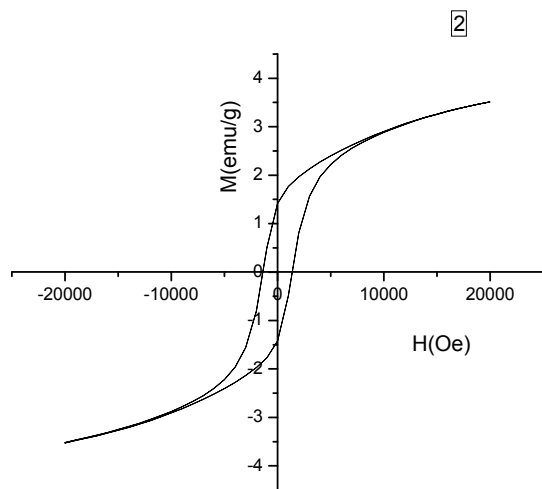


**Fig7.6: Magnetic hysteresis loop of  $\text{Sr}_{0.6}\text{Pr}_{0.4}\text{Fe}_{11.6}\text{Co}_{0.4}\text{O}_{19}$  at pH=2**

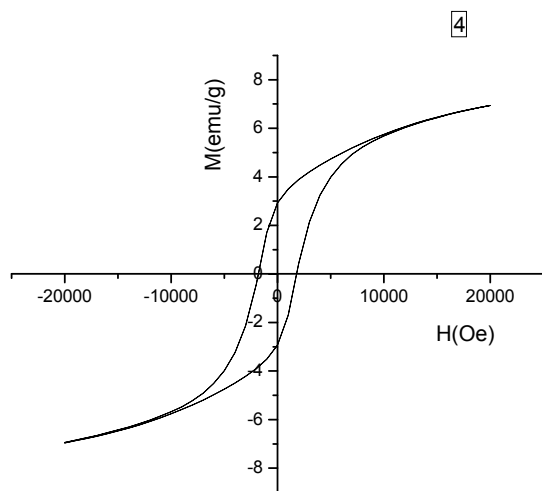


**Fig7.7: Magnetic hysteresis loop of  $\text{Sr}_{0.6}\text{Pr}_{0.4}\text{Fe}_{11.6}\text{Co}_{0.4}\text{O}_{19}$  at pH=4**

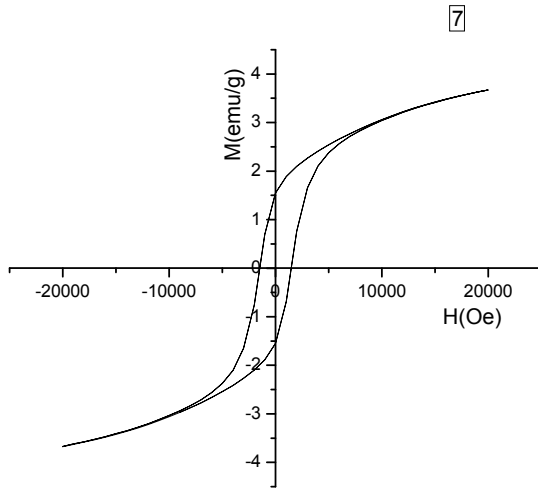


**Fig7.8: Magnetic hysteresis loop of  $\text{Sr}_{0.6}\text{Pr}_{0.4}\text{Fe}_{11.6}\text{Co}_{0.4}\text{O}_{19}$  at  $\text{pH}=7$**

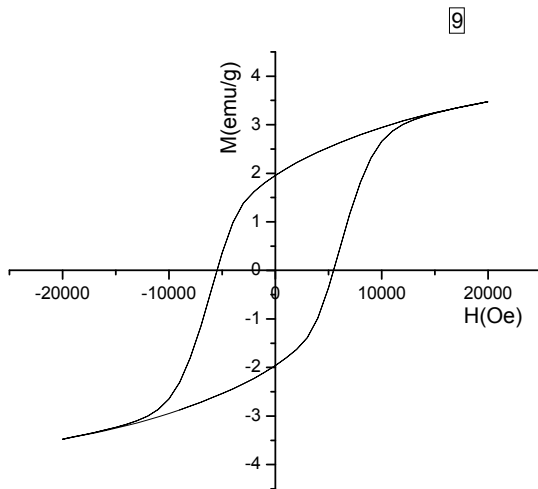


**Fig7.9: Magnetic hysteresis loop of  $\text{Sr}_{0.6}\text{Pr}_{0.4}\text{Fe}_{11.6}\text{Co}_{0.4}\text{O}_{19}$  at  $\text{pH}=9$**

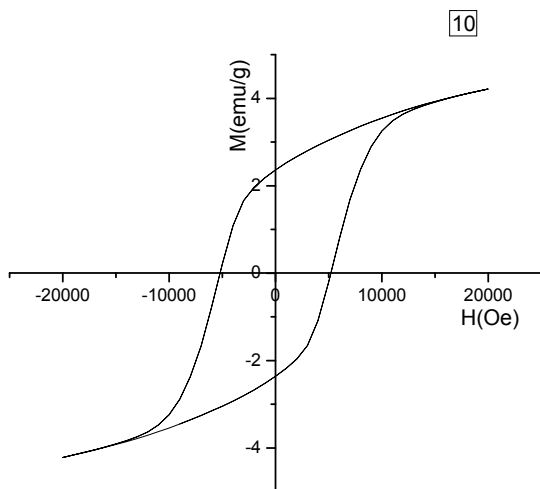


**Fig7.10: Magnetic hysteresis loop of  $\text{Sr}_{0.6}\text{Pr}_{0.4}\text{Fe}_{11.6}\text{Co}_{0.4}\text{O}_{19}$  at pH=10.47**

### **7.3.FOURIER TRANSFORM INFRARED SPECTROSCOPY (FT-IR):**

To find out the results of FTIR of the synthesized samples, it is compulsory to transform the powdered form of samples into thin pellets by using KBr press. To transform the powdered form of sample into thin pellets, a mixture of the sample and KBr, which is repeatedly taken in the ratio of 1:10 have been grinded with mortar and pestle. This mixture of sample was then pressed to create the thin pellet. The spectra of the samples were obtained in the range  $400$  to  $4000\text{cm}^{-1}$  with IR prestige-21 FTIR (model-8400S).

The bands in the range of  $400\text{-}600\text{ cm}^{-1}$  assigned to be for broadening of metal oxygen bond, the bands in the range of  $1500\text{-}2000\text{ cm}^{-1}$  indicates the presence of carboxylic acid, the peaks in the range of  $3000\text{-}3600\text{cm}^{-1}$  assigned for the  $\text{OH}^-$ , the peaks in the range of  $1400\text{-}1600\text{cm}^{-1}$  are assigned for the nitrate ions.

Bands in the range of  $1000\text{-}100\text{ cm}^{-1}$ , the IR bands of solids, are generally allotted to vibration of ions in the crystal lattice. But in our case mainly two broad metal-oxygen bands have been

seen in the IR spectra of ferrites. The maximum one generally located in the range of 600–550  $\text{cm}^{-1}$ , which is corresponded to the stretching vibrations of metal ions at the tetrahedral site, however the lowermost, detected in the range of 450–370  $\text{cm}^{-1}$  is allotted to stretching vibrations in octahedral sites.

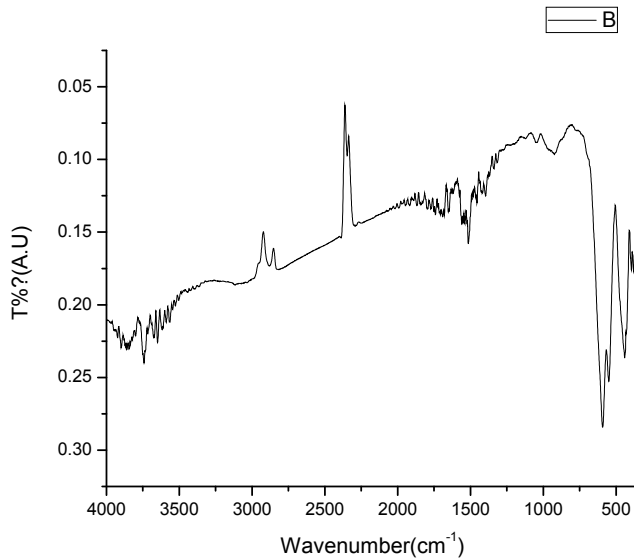


**Fig.7.11:FT-IR-Spectra of  $\text{Sr}_{0.6}\text{Pr}_{0.4}\text{Fe}_{11.6}\text{Co}_{0.4}\text{O}_{19}$  at  $\text{pH}=2$**

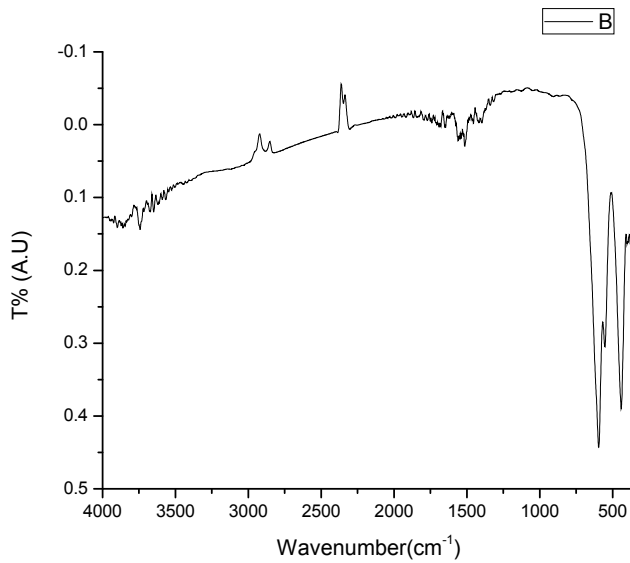


**Fig.7.12:FT-IR-Spectra of  $\text{Sr}_{0.6}\text{Pr}_{0.4}\text{Fe}_{11.6}\text{Co}_{0.4}\text{O}_{19}$  at pH=4**

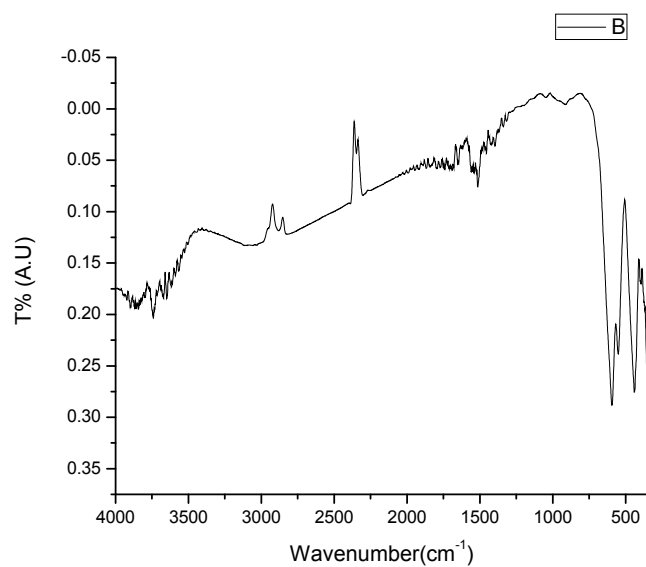


**Fig.7.13:FT-IR-Spectra of  $\text{Sr}_{0.6}\text{Pr}_{0.4}\text{Fe}_{11.6}\text{Co}_{0.4}\text{O}_{19}$  at pH=7**

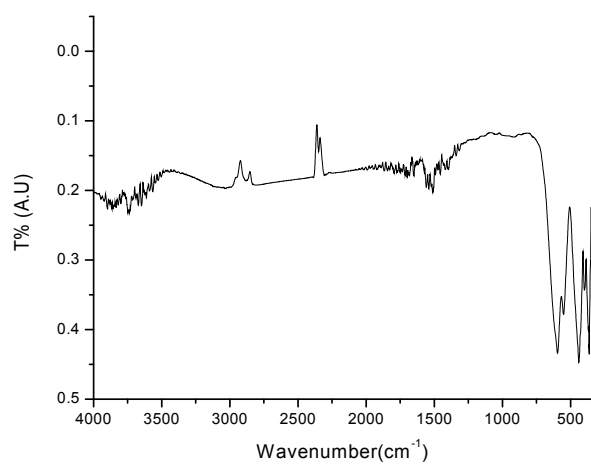


**Fig.7.14:FT-IR-Spectra of Sr<sub>0.6</sub>Pr<sub>0.4</sub>Fe<sub>11.6</sub>Co<sub>0.4</sub>O<sub>19</sub> at pH=9**

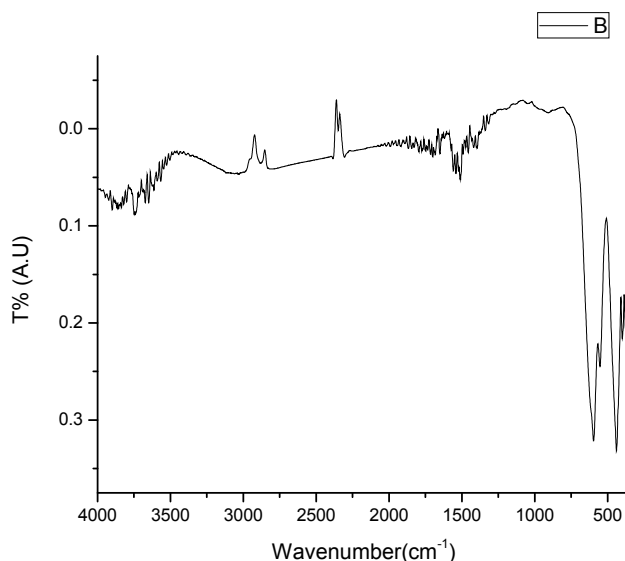


**Fig.7.15:FT-IR- Spectra of Sr<sub>0.6</sub>Pr<sub>0.4</sub>Fe<sub>11.6</sub>Co<sub>0.4</sub>O<sub>19</sub> at pH=10.47**

#### **7.4 THERMALGRAVIMETRY ANALYSIS (TGA):**

Figures below (Figs.7.16 and 7.17) are the DTA/TGA/DTG plot of the combustion product of the sample at pH=4 and pH=9. Thermogravimetric analyser (TGA) (Perkin Elmer Diamond TG/DTA) is used for thermal analysis under N<sub>2</sub> atmosphere with a heating rate of 10<sup>0</sup>C/min from 0 to 1000<sup>0</sup>C. It has been observed from DTA/TGA/DTG analysis that combustion reaction between the citric acid and metal nitrates occurred and all residue got burnt. There is an exothermic peak at 465<sup>0</sup>C for pH=4 and 645<sup>0</sup>C for pH=9 in differential thermogravimetry (DTG) plot which may be due to the decomposition of citric acid or may be due to the reaction between citric acid and nitrates. There are three essential steps in the formation of ferrite phase as per TG analysis: removal of water, organic compounds decomposition and crystallization. The weight loss of a precursor takes place in steps at 30<sup>0</sup>C-147<sup>0</sup>C, 147<sup>0</sup>C-328<sup>0</sup>C and 328<sup>0</sup>C-563<sup>0</sup>C for pH=4 and 52<sup>0</sup>C-208<sup>0</sup>C, 208<sup>0</sup>C-348<sup>0</sup>C and 348<sup>0</sup>C-665<sup>0</sup>C for pH=9 respectively. The weight loss of a precursor during exothermic reaction is due to the exclusion of water residues along with NO<sub>2</sub> and CO<sub>2</sub>. An additional weight loss of a precursor in the temperature range 411<sup>0</sup>C-563<sup>0</sup>C for pH4



and 413°C-662°C for pH9 can be attributed to the reaction between the intermediates for the formation of secondary phase along with the partial formation of hexaferrite. TG analysis shows no weight loss after 563°C(pH2) and 662°C(pH9), representing the completion of crystallization reaction. The DTA-curves in Figs. 7.16 and 7.17 illustrates the presence of both exothermic and endothermic effects in a precursor.

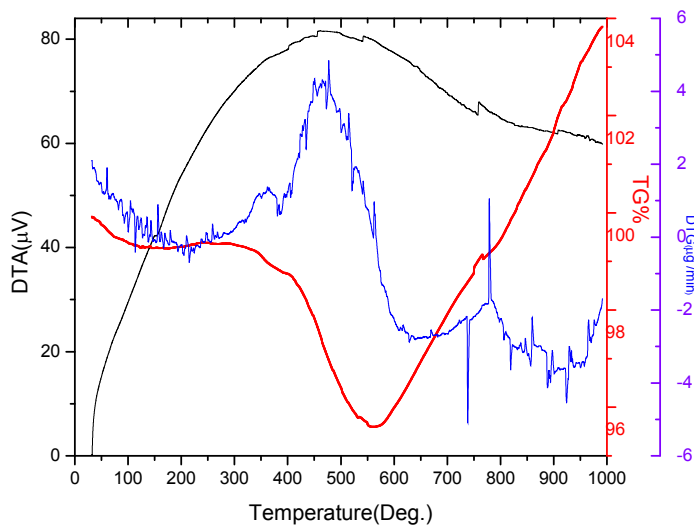


**Fig.7.16: TGA/DTG/DTA analysis of Sr<sub>0.6</sub>Pr<sub>0.4</sub>Fe<sub>11.6</sub>Co<sub>0.4</sub>O<sub>19</sub> at pH=4**

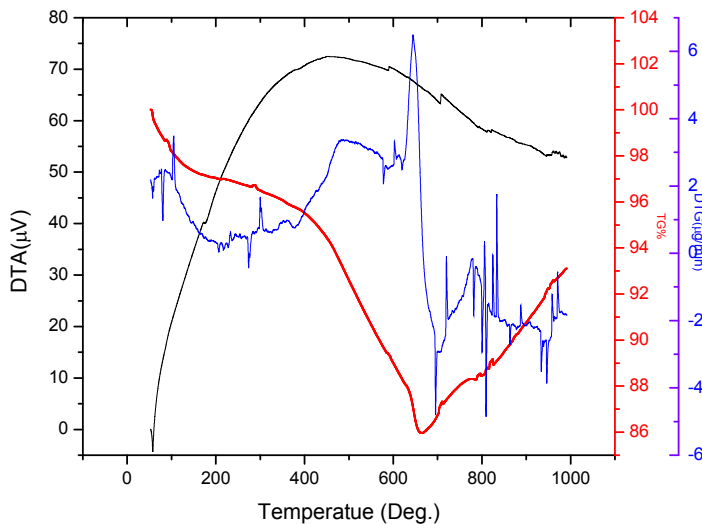


**Fig.7.17: TGA/DTG/DTA analysis of Sr<sub>0.6</sub>Pr<sub>0.4</sub>Fe<sub>11.6</sub>Co<sub>0.4</sub>O<sub>19</sub> at pH=9**

Magnetic nanoparticles exclusively hard nano ferrites have many applications in the field of permanent magnets, magneto-optic materials, microelectromechanical systems (MEMS), microwave devices and bio-medical. The physical and chemical properties of such nanoparticles mainly depend on the production method and chemical structure. In many applications, the particles size range from 1 to 100 nm. The main significance of the nanomaterial has three chief explanations:

- 1) Here is severe range of the nano structure, increasing properties like the physical property, extending from the naturally happening nanomagnets and they are very easy to form.
- 2) The involvement of nanoparticle effects in the improvement and explanation of the properties of innovative magnetic resources and
- 3) Nanomagnetism unlocks the entrance for innovative technologies.

The M-type nano-hexaferrites have been synthesized using sol-gel auto combustion technique and then characterized using XRD, FTIR and VSM. The XRD results of these studies confirmed the presence of hexagonal structure in prepared samples. The From TGA/DTA/DSC techniques, it was observed that the hexaferrite phase forms at a temperature of 800°C. The saturation magnetization, retentivity, coercivity and anisotropy are calculated using VSM.

## REFERENCES

1. Hasab, M.; Ebrahimi, S.A.; Badiei, A.; (2007); “Effect of different fuels on the strontium hexaferrite nanopowder synthesized by a surfactant-assisted sol–gel auto-combustion method”; *Journal of Non-Crystalline Solids*; **353**; 814–816
2. Jotania, R.B.; Khomane, R.B.; Chauhan, C.C.; Menon, S.K.; Kulkarni, B.D.; (2008); “Synthesis and magnetic properties of barium–calcium hexaferrite particles prepared by sol–gel and microemulsion techniques”; *Journal of Magnetism and Magnetic Materials*; **320**; 1095–1101
3. Bsoul, I. and Mahmood, S.H.; (2009); “Magnetic and structural properties of  $\text{BaFe}_{12-x}\text{Ga}_x\text{O}_{19}$  nanoparticles”; *Journal of Alloys and Compounds*; **489**; 110-114
4. Junliang, L.; Wei, Z.; Cuijing, G.; Yanwei, Z.; (2009); “Synthesis and magnetic properties of quasi-single domain M-type barium hexaferrite powders via sol–gel auto-combustion: Effects of pH and the ratio of citric acid to metal ions (CA/M)”; *Journal of Alloys and Compounds*; **479**; 863–869
5. Iqbal, M. and Ain, B.; (2009); “Synthesis and study of physical properties of  $\text{Zr}^{4+}$ - $\text{Co}^{2+}$  co-doped barium hexagonal ferrites” *Materials Science and Engineering B*; **164**; 6–11
6. Iqbal, M. and Farooq, S.; (2010); “Impact of Pr–Ni substitution on the electrical and magnetic properties of chemically derived nanosized strontium–barium hexaferrites”; *Journal of Alloys and Compounds*; **505**; 560–567
7. Liu, Y.; Drew, M.; Liu, Y.; Wang, J.; Zhang, M.; (2010); “Preparation, characterization and magnetic properties of the doped barium hexaferrites  $\text{BaFe}_{12-2x}\text{Co}_{x/2}\text{Zn}_{x/2}\text{Sn}_x\text{O}_{19}$ ,  $x=0.0$ – $2.0$ ”; *Journal of Magnetism and Magnetic Materials*; **322**; 814–818

8. Singhal, S.; Namgyal, T.; Singh, J.; Chandra, K.; Bansal, S.; (2011); "A comparative study on the magnetic properties of  $MFe_{12}O_{19}$  and  $MAFe_{11}O_{19}$  ( $M = Sr, Ba$  and  $Pb$ ) hexaferrites with different morphologies"; *Ceramic International*; **37**; 1833-1837
9. Sozeri, H.; Kucuk, I.; Ozkan, H.; (2011); "Improvement in magnetic properties of La substituted  $BaFe_{12}O_{19}$  particles prepared with an unusually low Fe/Ba molar ratio"; *Journal of Magnetism and Magnetic Materials*; **323**, 1799-1804
10. Davoodi, A.; Hashemi, B.; (2011); "Magnetic properties of Sn-Mg substituted strontium hexaferrite nanoparticles synthesized via coprecipitation method"; *Journal of Alloys and Compounds*; **509**; 5893-5896
11. Nakamura, Shin; Tsunoda, Yorihiro; Fuwa, Akio; (2012) " Mossbauer study on Y-type hexaferrite  $Ba_2Mg_2Fe_{12}O_{22}$ "; *Hyperfine Interactions*; **208**; 49-52
12. Wang, Zhanyong; Zhou, Zhipeng; Zhang, Weirong; Quian, Huichun; Jin, Minglin; (2013) "Preparation and Magnetic Properties of  $Nd^{3+}$ ,  $Al^{3+}$ ,  $Ca^{2+}$  substituted M- Type Strontium Hexaferrites"; *Journal of Superconductivity and Novel Magnetism*; **26**; 3501-3506
13. Xu Fenfang, Ma Li, Gan Mengyu , Tang Jihai, Li Zhitao, Zheng Jiyue , Zhang Jun, Xie Shuang, Yin Hui, Shen Xiaoyu, Hu Jinlong, Zhang; (2014) "Preparation and characterization of chiral polyaniline/barium hexaferrite composite with enhanced microwave absorbing properties"; *Journal of Alloys and Compounds*; **593**; 24-29
14. Kaur Talwinder; (2015) "Effect of calcination temperature on microstructure, dielectric, magnetic and optical properties of  $Ba_{0.7}La_{0.3}Fe_{11.7}Co_{0.3}O_{19}$  hexaferrites; *Physica B*; **456**; 206-212

15. Kaur Talwinder et al., (2015) “Effect on dielectric, magnetic, optical and structural properties of Nd–Co substituted barium hexaferrite nanoparticles” *Applied Physics A*, (DOI: 10.1007/s00339-015-9134-z)

## ABSTRACT

**Name:** Sonam Chauhan

**Reg. No.:** 11302052

**Session:** 2013- 2015

**Degree:** M.Sc.(Hons)

**Major:** Physics

**Department:** Physics

**Project Title:** Effect of pH on structural and magnetic properties of Pr-Co substituted Strontium Hexaferrite.

**Guide:** Dr A.K. Srivastava

M-type barium hexaferrite powder have been synthesized using sol gel auto combustion method. The pH values (pH= 2, 4, 7, 9 and 10.47 ) of the ferrite are controlled by the ammonia solution. X ray -diffraction (XRD) powder patterns of the samples show the formation of pure phase of M-type hexaferrite after pH 7. The presence of two prominent peaks, at  $438\text{ cm}^{-1}$  and  $596\text{ cm}^{-1}$  in Fourier Transform Infrared Spectroscopy (FT-IR) spectra, gives the idea of formation of M-type hexaferrites. The M-H curve obtained from Vibrating Sample Magnetometer (VSM) are used to calculate saturation magnetization ( $M_s$ ), retentivity ( $M_r$ ),and coercivity ( $H_c$ ). The maximum value of coercivity ( $5432\text{ Oe}$ ) is found at  $\text{pH} = 9$ . The maximum retentivity is found  $2.8979\text{ emu/g}$  at  $\text{pH} = 4$ .